

AD-A186 021

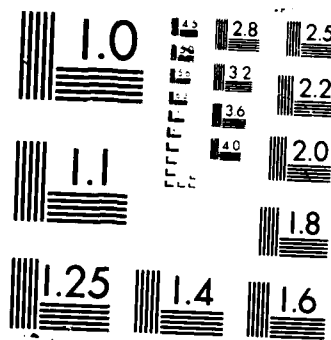
TEXTURE STUDY OF SYNTHETIC APERTURE RADAR (SAR) IMAGES 1/1  
OF OCEAN SURFACES(U) NAVAL RESEARCH LAB WASHINGTON DC  
L DU 20 AUG 87 NRL-MR-6005

UNCLASSIFIED

F/G 17/9

NL





REOCOPY RESOLUTION TEST CHART

**Naval Research Laboratory**

Washington, DC 20375-5000

2



NRL Memorandum Report 6005

**AD-A186 021**

**DTIC FILE COPY**

**Texture Study of Synthetic Aperture Radar (SAR)  
Images of Ocean Surfaces**

LI-JEN DU

*Systems Control and Research Branch  
Radar Division*

August 20, 1987

*\*Original contains color  
plates: All DTIC reproduct-  
ions will be in black and  
white\**

**DTIC**  
**ELECTE**  
**S** OCT 19 1987 **D**  
**D**

87 10 2 076

## REPORT DOCUMENTATION PAGE

1a. REPORT SECURITY CLASSIFICATION UNCLASSIFIED		1b. RESTRICTIVE MARKINGS	
2a. SECURITY CLASSIFICATION AUTHORITY		3. DISTRIBUTION/AVAILABILITY OF REPORT Approved for public release; distribution unlimited.	
2b. DECLASSIFICATION / DOWNGRADING SCHEDULE			
4. PERFORMING ORGANIZATION REPORT NUMBER(S) NRL Memorandum Report 6005		5. MONITORING ORGANIZATION REPORT NUMBER(S)	
6a. NAME OF PERFORMING ORGANIZATION Naval Research Laboratory	6b. OFFICE SYMBOL (if applicable) Code 5380	7a. NAME OF MONITORING ORGANIZATION	
6c. ADDRESS (City, State, and ZIP Code) Washington, DC 20375-5000		7b. ADDRESS (City, State, and ZIP Code)	
8a. NAME OF FUNDING / SPONSORING ORGANIZATION Office of Naval Research	8b. OFFICE SYMBOL (if applicable) ONR	9. PROCUREMENT INSTRUMENT IDENTIFICATION NUMBER	
8c. ADDRESS (City, State, and ZIP Code) Arlington, VA 22217		10. SOURCE OF FUNDING NUMBERS	
11. TITLE (Include Security Classification)			
Texture Study of Synthetic Aperture Radar (SAR) Images of Ocean Surfaces			
12. PERSONAL AUTHOR(S) Du, Li-jen			
13a. TYPE OF REPORT Interim	13b. TIME COVERED FROM _____ TO _____	14. DATE OF REPORT (Year, Month, Day) 1987 August 20	15. PAGE COUNT 29
16. SUPPLEMENTARY NOTATION			
17. COSATI CODES		18. SUBJECT TERMS (Continue on reverse if necessary and identify by block number)	
FIELD	GROUP	SUB-GROUP	Texture Synthetic aperture radar Co-occurrence Ocean surface Probability matrix
19. ABSTRACT (Continue on reverse if necessary and identify by block number)			
<p>This report describes the first phase of a study whose objective is to establish the relation between the texture in SAR images of the ocean surface and the relevant physical conditions giving rise to this texture.</p> <p>The initial concern is the selection of a technique which leads to a reliable separation of images into regions of different texture. Section II of the report discusses the role of texture in image analysis. Section III introduces the concept of a feature and establishes rationale for the selection of gray level co-occurrence matrix approach to feature extraction. Section IV describes the proposed classification algorithm and Section V gives the results for several test images.</p> <p>It is found that this approach works well in classification of land scenes. For ocean images which exhibit only subtle differences between regions the approach's discriminating power is less satisfactory than for land scenes. In Section VI alternate approaches are suggested for ocean images.</p>			
20. DISTRIBUTION/AVAILABILITY OF ABSTRACT <input checked="" type="checkbox"/> UNCLASSIFIED/UNLIMITED <input type="checkbox"/> SAME AS RPT <input type="checkbox"/> DTIC USERS		21. ABSTRACT SECURITY CLASSIFICATION UNCLASSIFIED	
22a. NAME OF RESPONSIBLE INDIVIDUAL Li-jen Du		22b. TELEPHONE (Include Area Code) (202) 767-2003	22c. OFFICE SYMBOL Code 5380

## CONTENTS

I.	INTRODUCTION .....	1
II.	TEXTURE APPROACH TO IMAGE ANALYSIS .....	4
III.	TEXTURE FEATURES EXTRACTION FROM SPATIAL GRAY-TONE CO-OCCURRENCE MATRIX .....	5
IV.	IMAGE CLASSIFICATION ALGORITHM .....	8
V.	CLASSIFICATION RESULTS .....	11
VI.	CONCLUSIONS AND DISCUSSIONS .....	22
	REFERENCES .....	23

Accumulation For	
NTIS CP221	<input checked="" type="checkbox"/>
DTIC TAB	<input type="checkbox"/>
Other Agencies	<input type="checkbox"/>
Classification	
By	
Classification	
Authorization	
Serial Number	
Date	
A-1	



## Texture Study of Synthetic Aperture Radar(SAR) Images of Ocean Surfaces

### I. INTRODUCTION

Microwave oceanography is a relatively new field of research in which established active and passive microwave technologies are being used to explore various ocean properties. One area of practical interest in this effort is the search for methods to acquire measurements which would allow an estimation of the wind field, wave field, and meteorological conditions on the ocean surface. This report is related to the segmentation of synthetic aperture radar(SAR) images into areas where significant difference in surface wave patterns existed at the time when the images were taken.

Experimental observations conducted in recent years have verified the fact that ocean surface waves and patterns can be detected in SAR images[1-5]. The basic physical principle of SAR imaging is that the backscattered microwave energy from a

reflecting area sensed by the radar receiver contains information on the roughness of that area. However, a SAR image is generated by making use of the coherent Doppler information associated with the motion of the radar relative to the target. Any unaccounted for motion displaces the image of a target from its true position. For a target such as the ocean surface, exhibiting movements in several directions and on different scales, image blurring occurs making various ocean features less visible to the interpreter. As a consequence, there is no complete SAR imaging theory to adequately describe the response of a synthetic aperture radar to changes in the reflectivity of the surface of the ocean.

A Radar image is a two-dimensional map of the variation in the local coherent backscattering cross-section of the illuminated target surface. For ocean images, these changes will depend upon the changes of local surface tilt angle, variation of its roughness, height and size of the waves, the wave's velocity and its direction, the polarization of the radar waves, radar wavelength, viewing geometry, uncompensated platform acceleration, etc. The wave velocity affects the image in an indirect and complex way because of the way the image is generated[6,7]. The process involved is not fully understood. In addition, it is difficult to make the simultaneous measurements to find sufficient ground truth over a significantly broad

area within the image. Hence, there is still no acceptable procedures which can be relied upon to generate an accurate estimate of ocean wave spectra from SAR image intensity data [8-11].

Since a direct estimation of the relevant environmental conditions is difficult to achieve, an indirect approach of segmenting the SAR image into areas with clearly different environmental conditions can be a meaningful alternative for ocean surface remote sensing. Tonal classifiers that were successful in discriminating areas of different characteristics in multispectral scanner(MSS) Landsat imagery of land scenes do not produce good results when applied to radar images. The main difficulty is due to the effect of speckle, a coherent noise phenomenon associated with all coherent sensors, which tends to reduce interpretability of the image. For radar images, texture analysis which examines the intrinsic spatial variability has turned out to be a more viable approach in discriminating among different land-use types and geological formations[12-14]. Based on this experience, an attempt has been made to study the relation between the texture in a SAR image of ocean surface and the relevant physical conditions giving rise to this texture, namely the wave field and indirectly the wind field.

## II. TEXTURE APPROACH TO IMAGE ANALYSIS

Texture is an intrinsic characteristic which exists in virtually all types of images. It has been a subject of study in image analysis and classification for over two decades. Although it is easy for anyone to recognize its existence and describe its structure in simple terms, the meaning of texture has not been precisely defined nor has a general analytical technique to extract numerical measure of it from image data been established[15]. Mapping semantic expressions into precise language and the appropriate equivalent mathematical formulation can be difficult. Basically texture concerns the pixel variation within a neighbourhood in an area which constitutes a small part of the whole image.

The problem may be viewed from two aspects. In the first aspect, it deals with the tonal primitives or local properties and in the second aspect it deals with the spatial organization of these tonal primitives. Tonal primitives are regions with special tonal properties such as the average and/or the range value of the tone level. The area covered by these regions are composed of all the connected pixels with a similar property. The spatial organization may be random, or have specific structural or probabilistic inter-dependence among neighboring primitives. Methods developed for studying texture have to address both aspects of the problem. There have been

many statistical and structural approaches developed to measure and characterize image texture[15]. However, each approach emphasized a specific narrow aspect of a problem for which a certain measure of success was achieved. Yet for other images the same approach shows serious weaknesses and limitations. Among the approaches available we selected the spatial gray tone co-occurrence probability matrix approach to extract textural properties from blocks of the SAR image data. This approach's power lies in its computational simplicity and its invariance properties under monotonic gray tone transformation. It has been applied quite successfully in classifying photomicrographic images[16], in identifying objects or regions of interest in LANDSAT optical images[17,18], and recently in land-use and sea-ice type discrimination of SAR images[13,19].

### III. TEXTURE FEATURES EXTRACTION FROM SPATIAL GRAY-TONE CO-OCCURRENCE MATRIX

The spatial gray-tone co-occurrence matrix method of extracting texture properties from images is based upon the assumption that the texture information in an image is contained in the overall or average spatial relationship which the neighborhood pixel gray tones maintain with respect to each other. In the first step, a set of probability matrices are evaluated by

scanning through a given block of the image. The next step is to evaluate a set of feature values based on a properly chosen formula with the elements in these matrices as the arguments. Feature values are numerical descriptors which characterize the statistical or structural nature of the texture by specific numbers. Feature values obtained from known samples are used in the classifier design. Feature values evaluated from unknown image blocks are used for image category discrimination.

The gray-tone co-occurrence matrix of an image block is defined as follows. Suppose the image block to be analyzed for texture is rectangular and has  $N_c$  resolution cells in the horizontal direction, and  $N_r$  resolution cells in the vertical direction. The gray tone of each cell is quantized into  $N_g$  steps. The whole image block is digitized as a two dimensional function of  $N_r$  by  $N_c$  cell data. The dimension of the matrix equals  $N_g$ . Its elements are the relative frequencies or probabilities  $p_{i,j}$ . The quantity,  $p_{i,j}$ , denotes the probability of the two neighboring cells having gray tones of  $i$  and  $j$  respectively. Quantities  $i$  and  $j$  take on integer values in the range from zero to  $N_g - 1$ . These matrices are symmetric and are also functions of the separation distance between the two cells as well as the direction of their separation. The distance is counted in terms of the numbers of cells separating the two. Usually there are four angular directions to be considered which are the horizontal, vertical, lower left and upper right, and lower right and upper left. Many types of textural features can

be extracted from these matrices[17]. They are defined by the familiar statistical terminology with the corresponding formulas using the matrix elements as arguments instead of the usual data samples. The special physical meaning of each of these features as related to the image data composition structure can be visualized by carefully examining its formula definition. Since there are many possible choices of feature definitions, not all will be independent. The following features have been mentioned by many investigators and are employed in this study:

1) Uniformity

$$f_1 = \sum_i \sum_j p_{i,j}^2, \quad (1)$$

2) Contrast

$$f_2 = \sum_i \sum_j (i-j)^2 p_{i,j}, \quad (2)$$

3) Entropy

$$f_3 = - \sum_i \sum_j p_{i,j} \log p_{i,j}, \quad (3)$$

4) Inverse Difference Moment

$$f_4 = \sum_i \sum_j p_{i,j} / [1 + (i-j)^2] \quad (4)$$

### 5) Correlation

$$f_s = [\sum_i \sum_j (ij)p_{i,j} - \mu_i \mu_j] / \sigma_i \sigma_j \quad (5)$$

where

$$\mu_i = \sum_j i p_{i,j}$$

$$\mu_j = \sum_i j p_{i,j}$$

$$\sigma_i^2 = \sum_j i^2 p_{i,j} - (\sum_j i p_{i,j})^2$$

$$\sigma_j^2 = \sum_i j^2 p_{i,j} - (\sum_i j p_{i,j})^2$$

## IV. IMAGE CLASSIFICATION ALGORITHM

With only a limited number of samples available for training purposes, and a set of features whose probability density functions are too difficult to be estimated, pattern classifier based on Bayes likelihood ratio test can not be constructed. A simpler and more feasible procedure to handle this problem is to find a linear discriminant function based on a minimum mean-square error approach[20,21]. In this approach only a finite number of available training samples are assumed and the

discriminant function  $h(z)$  separating two classes becomes simply

$$h(Z) = W^T Z \quad (6)$$

where  $T$  indicates the transpose of the vector  $W$  and  $Z$  is the modified sample vector of  $n$  feature components with the form

$$Z = (1 \ f_1 \ f_2 \ f_3 \ - \ - \ - \ - \ f_n)^T \quad (7)$$

The linear vector  $W$  is defined by

$$W = (U \ U^T)^{-1} U \Gamma \quad (8)$$

where  $U$  is a matrix constructed of the training sample feature vectors and has the following form,

$$U = \begin{bmatrix} 1 & 1 & -1 & -1 \\ f_{1,1} & f_{N_1,1} & -f_{N_1+1,1} & -f_{N_1+N_2,1} \\ \vdots & \vdots & \vdots & \vdots \\ f_{1,n} & f_{N_1,n} & -f_{N_1+1,n} & -f_{N_1+N_2,n} \end{bmatrix} \quad (9)$$

$N_1$  and  $N_2$  are the number of the samples in the class 1 and class 2 respectively. The first subscript in the matrix elements of (9) refers to the sample sequence number and the second subscript refers to the texture feature sequence number. The vector  $\Gamma$  has components which are the assumed desired output of the function

$h(z)$  for the training samples in (6).

$$\Gamma(z) = [\gamma(z_1) \dots \gamma(z_{n_1+n_2})]^T \quad (10)$$

In the work reported here, all the components in (10) are assumed to be 1.0. For a feature vector obtained from an image block of class 1, the discrimination function  $h(z)$  will yield a positive result close to 1.0. A feature vector evaluated from data in image block of class 2 will yield a negative result close to -1.0.

In the multicategory cases, linear vector  $w$  is evaluated from training sample data for each possible pair of classes. For an image block of unknown class to be classified, its feature vector is tested against all the linear vectors in (6). The class which scores the highest is the category to which the unknown block is assigned. If there is a tie between two classes, the result of the discrimination function with the vector  $w$  made from these two classes settles the ambiguity. If there are more than two classes with the same score in the classifying process, an undecided case appears. This situation can happen if more than three classes exist.

## V. CLASSIFICATION RESULTS

The images being used to test the classification algorithms are shown in Figures 1a, 2a, and 3a. Figure 1a shows the image of Chesapeake bay generated by appropriate processing of the Seasat-A SAR video signal. It was taken on August 5, 1978. Figures 2a and 3a are sub-images obtained during the SIR-B mission on October 11, 1984. They cover the ocean surface outside the U. S. east coast. The area shown in Figure 2a is centered around the geographical location at 37° North and 74° West. Figure 3a shows the image of New York Bight/Hudson canyon area. All 3 images have the size of 512 by 512 pixels(resolution cells).

In our classification experiments with the image of Fig. 1a, several sub-images of size 32 by 32 resolution cells are chosen within the image as the training samples. Linear vector functions  $W$  were derived from the feature data which are average values in four directions of uniformity, contrast, correlation, and entropy. Four categories of land use were chosen in this image. They are the water, rural area, small town urban area, and man-made structures such as, the bridges. Four or five training samples were selected for every category. In the classifying process, a window of 33 by 33 pixels is scanned through the whole image starting at the upper left corner. The texture features evaluated with the pixel data within each window were

used in equations (6) and (7) to determine the category of this window. A new image shown in Fig. 1b was created with the pixel location corresponding to the center of this window assigned a chosen tone level for that category. This image has a size of 496 by 496 pixels since the 16 pixels along the edge could not be classified. The chosen pixel tone levels are 0, 50, 150, 200 for water, rural area, small town urban area, and the man-made structure respectively. The undecided pixels were assigned a level of 255. To enhance the distinction between these categories for viewing, pseudo-color was used with dark blue corresponding to zero pixel value and bright red corresponding to the maximum pixel value of 255. With this color coding, the water category appears as black, rural area appears as light blue, small town as green and man-made structure as orange. The undecided pixels show red color. By comparing Figures 1a and 1b, it is evident that co-occurrence matrix method of generating texture features for image classification yields excellent results. This image was used as a sample to test the power of this classification approach and to check the accuracy of the algorithms and programs developed.

The image shown in Fig. 2a is a difficult one to classify. In some parts of the image, the pixel's intensity variations reveal directional streaks as compared with other parts where it is more or less homogeneous. The areas with the streaks indicate the regions on the ocean surface where stronger waves and winds may exist. Our objective was to develop the al-

gorithms and programs which will enable us to use the computer to map the image automatically into streak and non-streak areas. Since regions with the same textural properties cover broader area in this image, a larger size of 64 by 64 pixels was chosen for the training sample. About four or five of both categories were selected. Features of uniformity, contrast, entropy, inverse difference moment, and correlation in all four directions were evaluated. A pair among these five which showed consistent and greatest percentage difference in all four directions between these two categories of training samples was chosen as the feature vector components in equations (7) and (9). Figure 2b shows one of the better results obtained. The image in Figure 2a was divided into 64 subimages of 64 by 64 pixels each. Pixel data in each sub-image were used to determine that sub-image's classification. The blank cells in Figure 2b indicate that the corresponding sub-images in Figure 2a were classified as region without streaks and those cells labeled with letter S indicate sub-images classified as region with streaks. The training samples chosen do not coincide with any one of these sub-images. Our subjective judgement of the classification accuracy is that it is 60% to 70%, based on careful examination of these sub-images.

The image in Figure 3a was classified in a way similar to that of the image in Figure 2a. Three classes of training samples were chosen. The first two classes are the same as those chosen from image in Fig. 2. The third class training samples



Fig. 1a - Seasat-A SAR image of Chesapeake bay on Aug. 5, 1978



Fig. 4b - Classified image with 4 classes of  
land use of image in Fig. 4a

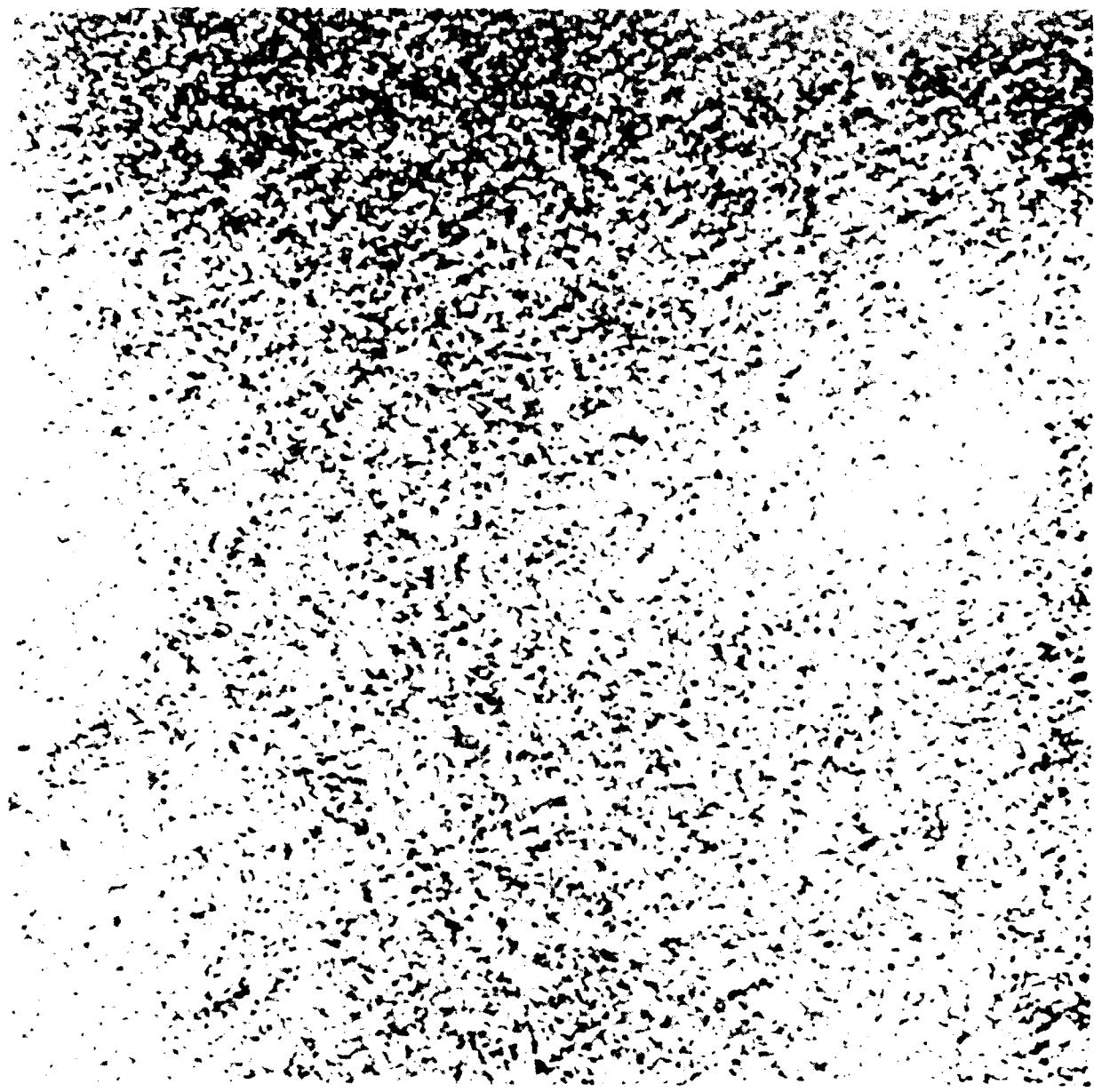


Fig. 2a — SIR-B image of ocean surface around geographic location of 37°N and 74°W.

		S		S				
			S		S	S		
					S	S	S	
S			S	S	S	S		
			S			S	S	
				S			S	
			S		S	S		
				S	S			S

Fig. 2b — Classified image with 2 different regions of surface meteorological conditions of image in Fig. 2a.

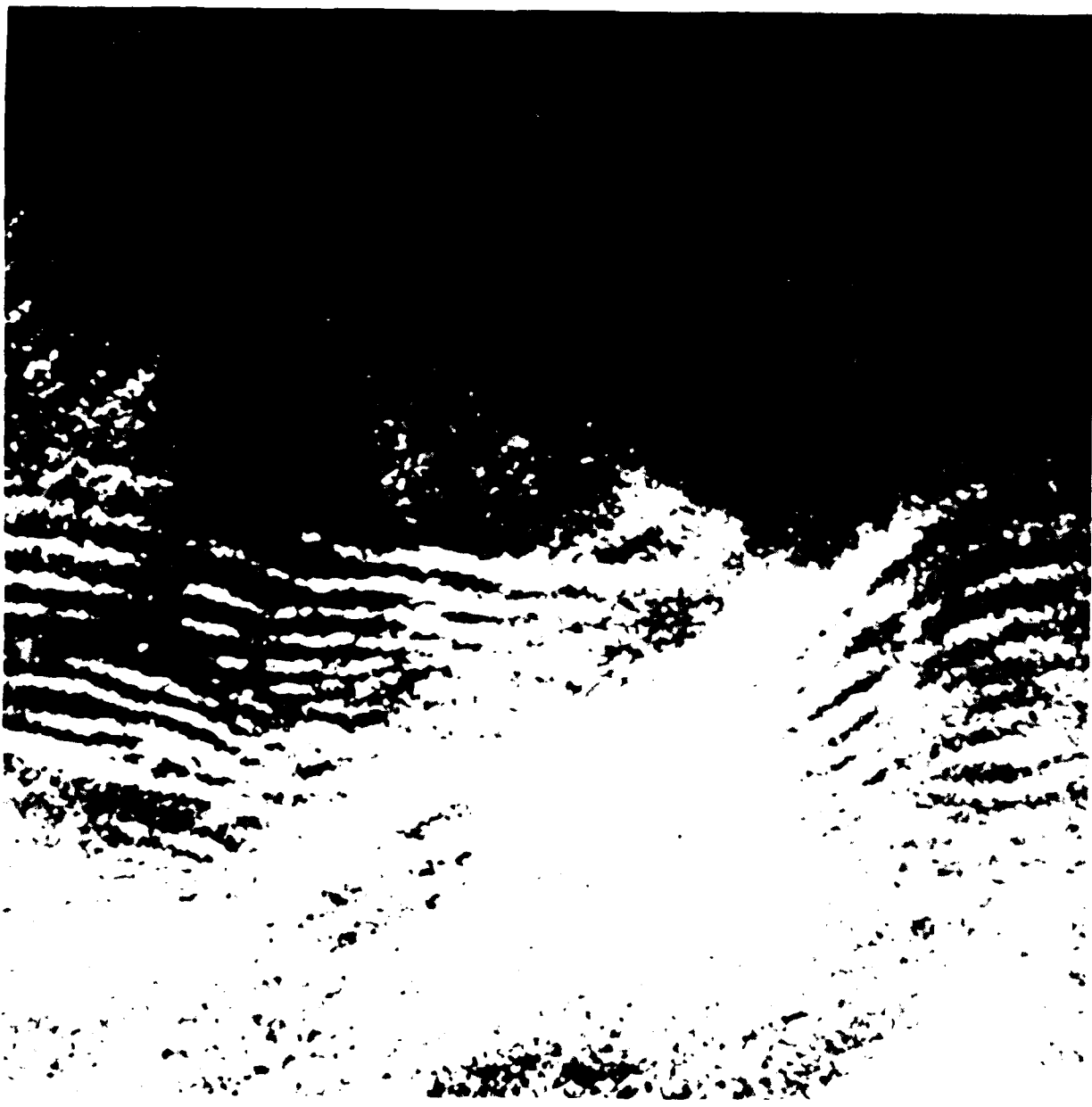


Fig. 3a - SIR-B image of ocean surface at New York/Hudson canyon area.

LS				SS	SS	SS	SS	
LS		LS	SS	LS	SS	SS	LS	
SS	SS	SS	LS	SS	SS	LS	LS	
SS	LS	LS	SS	LS	SS	LS	LS	
SS	LS	SS	LS	LS	LS	LS	LS	SS
LS	SS	SS	SS	LS	SS	LS	LS	
LS	LS		SS	LS		SS	LS	
LS			LS	LS			LS	

Fig. 3b — Classified image with 3 different regions of surface meteorological conditions of image in Fig. 3a.

were selected in Figure 3a in the areas where large size streaks are evident. Since the intensity level of the pixels in Figure 3a varies over much broader range than that of Figure 2a, mean values of each sub-image were re-adjusted to equal the level of one of the training samples of Figure 2 before feature values were evaluated for both the training and classifying process. Figure 3b shows one of the better results. The blank cells and the cells labeled SS indicate the corresponding sub-images in Figure 3a which were classified as belonging to the same classes of non-streak and streak regions as those in Figures 2. The cells labeled LS indicate that the corresponding sub-images were classified as regions with large streaks. Again, subjective evaluation of the result indicates a classification accuracy of around 70%. This is much better than we achieved for the image of Figure 2, because this is a three class problem as compared with that of a two class one. However, it is apparent that the image of Figure 3a is one which should be much easier for class separation. The results of classifying Figures 2a and 3a are not as good as was expected. No attempt was made to classify each pixel and generate a new image as was done in creating the image in Figure 1b for the image in Figure 1a. It is anticipated that a clear partition of the image into two or three classes of regions is unlikely.

## VI. CONCLUSIONS AND DISCUSSIONS

This effort in the texture study of SAR images confirms the fact that the texture features derived from co-occurrence matrix method are quite powerful in land use or terrain classifications of radar images. The method's applicability to images of the ocean surface is still under investigation. Ocean images generally fall into two classes. Those that exhibit only subtle differences in texture between different regions and those that show more pronounced differences. For the current work we have deliberately selected imagery in the first category. It is apparent that for such images the method's discriminating power is less effective than for images of land scenes. It is conceivable that a different combination of features or parameters in the matrices may to some extent improve this situation. However, a truly significant improvement in its texture distinguishing capability for images in the first category may not be possible. In this case, to continue the goal of separating ocean surface SAR image into regions having different environmental conditions through texture study, a different approach may have to be pursued. The approaches will be tried which seemed to have worked well on similar problems as shown by recent investigations. These are, the texture energy measure approach[22,23], the Fourier analysis texture feature extraction approach[24], and the non-linear transformation of local patterns approach[25]. As far as the second category of images is concerned, typical imagery is being collected and it will be used for a further evaluation of the co-occurrence matrix approach.

### References

- [1] L. I. Moskowitz, "The feasibility of ocean current mapping via synthetic aperture radar methods," *Proc. Fall Conv. Amer. Soc. Photogrammetry*, pp. 760-771, Oct. 1973.
- [2] T. R. Larson and J. W. Wright, "Imaging ocean current gradients with synthetic aperture radar," *URSI Fall meeting*, Boulder, CO, 1974.
- [3] W. E. Brown, Jr., C. Elachi, and T. W. Thompson, "Radar imaging of ocean surface patterns," *J. Geophys. Res.*, vol. 81, pp. 2657-2667, 1976.
- [4] C. Elachi, "Wave patterns across the north Atlantic on September 28, 1974, from airborne radar imaging," *J. Geophys. Res.*, vol. 81, pp. 2655-2656, 1976.
- [5] C. Elachi and W. E. Brown, "Models of radar imaging of the ocean surface waves," *IEEE Trans. on Antenna and Propagation*, vol. AP-25, pp. 84-95, 1977.
- [6] A. W. Rihaczek, *Principles of High Resolution Radar*. New York, NY: McGraw-Hill, 1969.
- [7] R. O. Harger, *Synthetic Aperture Radar Systems*. New York: Academic, 1970.

- [8] W. Alpers, D. B. Ross, and C. L. Rufenach, "On the detectability of ocean surface waves by real and synthetic aperture radar," *J. Geophys. Res.*, vol. 86, pp. 6481-6498, 1981.
- [9] W. Alpers, "Monte Carlo simulation for studying the relationship between ocean wave and synthetic aperture radar image spectra," *J. Geophys. Res.*, vol. 88, pp. 1745-1759, 1983.
- [10] F. M. Monaldo and D. R. Lyzenga, "On estimation of wave slope- and height-variance spectra from SAR imaging," *IEEE Trans. Geosci. and Remote Sensing*, vol. GE-24, pp. 543-551, 1986.
- [11] G. E. Keyte and J. T. Macklin, "SIR-B observations of ocean waves in the NE Atlantic," *IEEE Trans. Geosci. and Remote Sensing*, vol. GE-24, pp. 552-558, 1986.
- [12] F. T. Ulaby, F. Kouyate, B. Brisco and T. H. L. Williams, "Textural information in SAR images," *IEEE Trans. on Geosci. and Remote Sensing*, vol. GE-24, pp. 235-245, 1986.
- [13] K. S. Shanmugan, V. Narayanan, V. S. Frost, J. A. Stiles, and J. C. Holtzman, "Texture features for radar image analysis," *IEEE Trans. Geosci. and Remote Sensing*, vol. GE-19, pp. 153-156, 1981.

- [14] R. G. Blom and M. Daily, "Radar image processing for rock-type discrimination," *IEEE Trans. on Geosci. and Remote Sensing*, vol. GE-20, pp. 343-351, 1982.
- [15] R. M. Haralick, "Statistical and structural approaches to texture," *Proc. of the IEEE*, vol. 67, pp. 786-804, 1979.
- [16] R. M. Haralick and K. S. Shanmugan, "Computer classification of reservoir sandstones," *IEEE Trans of Geosci. Electron.*, vol. GE-11, pp. 171-177, 1973.
- [17] R. M. Haralick and K. S. Shanmugan, "Combined spectral and spatial processing of ERTS imagery data," *J. of Remote Sensing of the Environment*, vol. 3, pp. 3-13, 1974.
- [18] R. M. Haralick, K. S. Shanmugan, and I. Dinstein, "Textural features for image classification," *IEEE Trans. Syst. Sci. Cybern.*, vol. SMC-3, pp. 610-621, 1973.
- [19] Q. A. Holmes, D. R. Nuesch, and R. A. Shuchman, "Textural analysis and real-time classification of sea-ice types using digital SAR data," *IEEE Trans. Geosci. and Remote Sensing*, vol. GE-22, pp. 113-120, 1984.
- [20] K. Fukunaga, *Introduction to Statistical Pattern Recognition*. New York: Academic Press, 1972.

- [21] R. O. Duda and P. E. Hart, *Pattern Classification and Scene Analysis*. New York: John Wiley & Sons, 1973.
- [22] K. I. Laws, "Texture image segmentation," Image Processing Institute, University of Southern California, Rept. 940, Jan. 1980.
- [23] M. Pietikainen, A. Rosenfeld, and L. S. Davis, "Experiments with texture classification using averages of local pattern matches," *IEEE Trans. Syst., Man, Cybern.*, vol. SMC-13, pp. 421-426, 1983.
- [24] W. D. Stromberg and T. G. Farr, "A Fourier-based textural feature extraction procedure," *IEEE Trans. Geosci. and Remote Sensing*, vol. GE-24, pp. 722-731, 1986.
- [25] M. Ogata, M. Sekine and T. Musha, "Discrimination of radar clutter by texture analysis," *IEE Proceedings*, vol. 133, pt. F, no. 3, pp. 257-263, 1986.

END  
DATE  
FILMED  
DEC.  
1987